



Title	Global structure of Bidecadal precipitation variability in boreal winter
Author(s)	Minobe, Shoshiro; Nakanowatari, Takuya
Citation	Geophysical Research Letters, 29(10), 1396 <a href="https://doi.org/10.1029/2001GL014447">https://doi.org/10.1029/2001GL014447</a>
Issue Date	2002-05-15
Doc URL	<a href="http://hdl.handle.net/2115/20064">http://hdl.handle.net/2115/20064</a>
Rights	An edited version of this paper was published by AGU. Copyright 2002, American Geophysical Union, Geophysical Research Letters, Vol. 29-10
Type	article (author version)
File Information	GRL29-10.pdf



[Instructions for use](#)

# Global Structure of Bidecadal Precipitation Variability in Boreal Winter

Shoshiro Minobe<sup>1,2</sup> and Takuya Nakanowatari<sup>1</sup>

<sup>1</sup> Division of Earth and Planetary Sciences, Graduate School of Science, Hokkaido University, Sapporo, Japan.

<sup>2</sup> Frontier Research System for Global Change, Yokohama, Japan.

**Abstract.** Three global monthly precipitation datasets, including gauge measurements, gauge/satellite merged analysis (CMAP), and NCEP/NCAR reanalysis, are analyzed with respect to Bi-Decadal Oscillation (BDO) in boreal winter during the 20th century. Correlation and coherency analyses between the precipitations and the strength of the Aleutian low, which is an action center of the BDO, reveal substantial impacts of the BDO on precipitations around the Pacific Ocean. The covariability of the precipitations is prominent for Hawaii, mid-latitude eastern North America, Florida and eastern-China/Southern-Japan, and at some other regions including the Southern Hemisphere. The most coherent BDO precipitation pattern common to the CMAP and reanalysis features significant anomalies over the tropical (10°–30°N), central (30°–50°N) and northern (50°–70°N) North Pacific with alternating polarities. The influence of the BDO on Hawaii winter droughts and salinity in the North Pacific is discussed.

## Introduction

It is important to identify the rhythm of Earth's climate both because it helps us understand the cause of past climate changes and because of potential predictability of the climate variability in future. Recent studies revealed various decadal-to-centennial climate variations occurred in the 20th century (e.g., Mann and Park, 1996). One of the most prominent variations on these timescales is a quasi periodic oscillation on a 20-yr timescale, which distributes over both the Pacific and Atlantic Oceans with an action center in the North Pacific associated with the strength changes of the Aleutian low [e.g., White and Cayan, 1998], and is referred to as Bi-Decadal Oscillation (BDO) in the present paper. A number of papers are devoted to the discussion of the BDO in global- or Pacific-scale Sea-Level Pressure (SLP) and Surface Temperature (ST) fields [e.g., Ghil and Vautard, 1991; Mann and Park, 1996; White and Cayan, 1998; Tourre et al., 2000; Minobe et al., 2002]. Although it is not still clear whether the BDO arise from a single physical mechanism or multiple mechanisms, most of these studies showed similar spatial patterns in SLPs and STs over the North Pacific.

For precipitations, however, our understanding of their decadal-to-centennial variability is still poor. The global structure of bidecadal precipitation variability was not identified yet, though several regional analyses showed that precipitations varied on the bidecadal timescale in North America [e.g., Dettinger and Cayan, 1995; Cook et al., 1997; Cayan et al., 1998; Hu et al., 1998; Higgins and Shi, 2000] and Australia [Latif et al., 1997]. A better understanding of the precipitation changes on interdecadal timescales is clearly of scientific and social value. Here, we analyze global precipitation changes on the bidecadal timescale, by examining three precipitation datasets derived from gauge measurements, satellite observations and reanalysis, which provide complementary information.

## Data and methodology

Three gridded monthly precipitation datasets are analyzed in the present study. These datasets are land precipitations from gauge measurements (referred to as gauge data) [Dai et al., 1997], NCEP/NCAR reanalysis precipitations (referred to as reanalysis data) [Kalnay et al., 1996], and Climate Prediction Center satellite/gauge Merged Analysis of Precipitation (referred to as CMAP data) [Xie and Arkin, 1997]. The CMAP data used in the present study is a version in which the reanalysis precipitations were not incorporated. The periods of the records are 1900–1995, 1949–2000, and 1979–1999 for the gauge, reanalysis, and CMAP data, respectively. The grid size for the gauge and CMAP data is 2.5° in both longitude and latitude, and 1.875° in longitude and roughly 1.905° in latitude for the reanalysis data. We limit our attention to boreal winter data in the present paper, since it is known that the bidecadal atmospheric circulation changes are the most prominent in the winter season [Mann and Park, 1996; White and Cayan, 1998; Minobe et al., 2002].

The use of the multiple precipitation datasets is necessary to address the interdecadal precipitation changes. The gauge data have the longest availability, but they cover only a part of land. Although the reanalysis data have a complete spatial coverage, the quality of the reanalysis precipitations can be questionable, since the precipitations themselves were not assimilated [Kalnay et al., 1996]. The CMAP data are more reliable than the reanalysis data with almost complete spatial coverage, but the temporal availability is just one cycle of the BDO [Xie and Arkin, 1997]. Due to these intrinsic problems of the respective datasets, one cannot confidently estimate the interdecadal precipitation changes from none of the single precipitation dataset, but the complementary use of the three datasets taking account of the specific advantages and disadvantages is expected to provide the most useful information on the long-term changes of precipitations.

We estimated BDO signatures in the precipitation field by calculating correlation coefficients between precipitation time series at each grid and a representative time series for the BDO. As the representative BDO time series, we employ the 10–30-yr bandpass filtered wintertime (Dec.–Feb.) North Pacific Index (NPI). The NPI is a SLP time series averaged over a region from 30°–65°N, 160°E–140°W [Trenberth and Hurrell, 1994], which covers the area of high SLP-variability associated with the BDO, and represents interannual and decadal variability of the Aleutian low [Mann and Park, 1996; White and Cayan, 1998; Minobe et al., 2002]. The NPIs are calculated from 1899 to 2001 using an updated version of SLP dataset of Trenberth and Paolino [1980]. The major results of the present study are not changed, when we use as the representative BDO time series the first principal component of 10–30-yr filtered SSTs north of 20°N in the Pacific Ocean.

Significance of correlations is estimated by a Monte-Carlo simulation, using a phase randomization technique [Kaplan

and Glass, 1995]. In this method, absolute Fourier amplitudes (square root of spectra) for the NPI is estimated, and then 10,000 surrogate time series are generated by an inverse Fourier transform with the observed Fourier amplitudes and randomized phases. Surrogate correlation coefficients are estimated with the 10–30-yr bandpass filter between the surrogate NPI time series and an observed precipitation time series at each grid point. The relative position of the absolute value of the observed correlation coefficients in the sorted absolute values of the surrogate correlation coefficients gives the level of confidence for the observed correlation coefficient. This method takes into account of the influences of the bandpass filtering and also the intrinsic serial correlation of respective time series.

## Results

Correlations between the gauge precipitations and the NPI exhibit statistically meaningful positive or negative values around the Pacific Ocean (Fig. 1a). Positive correlations are observed over the eastern-China/southern-Japan, Hawaii, mid-latitude North America, Samoa Islands, southeastern Australia, and negative correlations are over Florida, and western Australia. The occurrence of significant correlations in the Southern Hemisphere is consistent with the previously reported observations that the BDO structure prevails the both hemispheres in ST and SLP fields [White and Cayan, 1998; Garreaud and Battisti, 1999]. Consequently, the BDO variability, represented by the strength changes of the Aleutian low, substantially influences global precipitation variability.

The frequency structure for the relation between the precipitation and the Aleutian low strength is examined by coherency analysis between the raw precipitation time series averaged over high correlation regions and the NPI (Fig. 2). The bidecadal coherency peaks significant at the 99% confidence level are evident for eastern-China/southern-Japan, Hawaii, mid-latitude eastern North America, and Florida at frequencies around 0.04–0.06 cycle yr<sup>-1</sup> (16–25-yr period), and those at the 95% confidence level are found for Samoa Islands, southwestern Australia and southeastern Australia. In these regions, the covariability between the precipitation and NPI is the most prominent at the bidecadal period on the decadal to centennial timescales. It is noteworthy that there are secondary coherency peaks around a 50-yr period at some locations (eastern-China/southern-Japan, mid-latitude eastern North America, and Samoa Islands), which may be related to a 50–70-yr oscillation over the Pacific Ocean [Minobe, 1997]. Minobe [1999; 2000] suggested that the superposition of the BDO and the 50–70-yr variability is the main body of the Pacific (inter-)Decadal Oscillation (PDO) proposed by Mantua *et al.* [1997]. For a recent review of the PDO, see Mantua and Hare [2002].

In order to fully understand the spatial structure of the BDO in precipitations, we employ NCEP/NCAR reanalysis precipitations. The most remarkable feature in the reanalysis correlations with the NPI (Fig. 1b) is the three broad patches over the North Pacific, with the positive correlations over the tropical (10°–30°N) and the northern (50°–70°N) North Pacific and negative correlations in the central North Pacific (30°–50°N). Another cluster of positive correlations is evident over eastern China.

Those features in the reanalysis correlations are essentially repeated in the correlations for the CMAP data (Fig. 1c), and hence the result of the CMAP data strongly supports the BDO structure obtained from the reanalysis data. An interesting

difference between the CMAP and reanalysis correlations is that the former have relatively strong negative correlations over Indian Ocean/Maritime Continent region than the reanalysis correlations. This difference is not due to the different periods of the data, since reanalysis correlations calculated for the period overlapping with the CMAP data are generally smaller than the CMAP correlations for this region. Therefore, the reanalysis is not likely to represent adequately the precipitation changes in the Indian Ocean/Maritime Continent region.

Additional support for the structure of the reanalysis correlations is given by the comparison with the correlations of the gauge data. The positive patches in the reanalysis correlations in the tropical and northern North Pacific covers Hawaii and western Alaska, respectively, where gauge data also indicate significant positive correlations. Moreover, the positive (negative) correlations are common in both the gauge and reanalysis data over eastern China (western Australia). Consequently, the correlation distribution of the gauge data supports some key features of the correlation distribution of the reanalysis data.

Among the regions where the strong correlations are commonly found in gauge, reanalysis and CMAP data, the largest explained variance by the 10–30-yr filtered NPI for 10-yr low-pass filtered precipitation time series is found at Hawaii (51%). The explained variance is a measure of the importance of the BDO, represented by the Aleutian low strength changes, in the precipitation changes on the timescales longer than the 10-yr period. As shown in Fig. 3, the time series of the wintertime Hawaii precipitation observed by gauge measurements has a prominent covariability with the NPI in regardless of whether or not the bandpass filtering is applied. The correlation between the unfiltered Hawaii precipitation time series and the NPI is as high as 0.71, indicating that 50% of the year-to-year variability of Hawaii wintertime precipitation is related with the strength changes of Aleutian lows (Fig. 3b). This relation appears to be stronger than the previously reported relation between Hawaii precipitation and El Niño/Southern Oscillation [e.g., Horel and Wallace, 1981; Ropelowski and Halpert, 1987; Chu, 1995], since the correlation between the raw precipitation and SOI remains 0.45, which explains only 20% of the year-to-year variance.

It is noteworthy that the reanalysis Hawaii precipitations are qualitatively consistent with the gauge data, but quantitatively underestimated on both the interannual and interdecadal timescales (Fig. 3). The standard deviations of gauge precipitations are 27 and 59 mm month<sup>-1</sup> with and without the bandpass filtering respectively, but the corresponding standard deviations of the reanalysis precipitations are as small as about 40% of the gauge standard deviations. The underestimation of the reanalysis precipitation is likely to be due to the coarse spatial resolution of the atmospheric model used for the reanalysis to resolve the effects of Hawaiian Islands, which play substantial roles in the atmosphere-and-ocean system [Xie *et al.*, 2001].

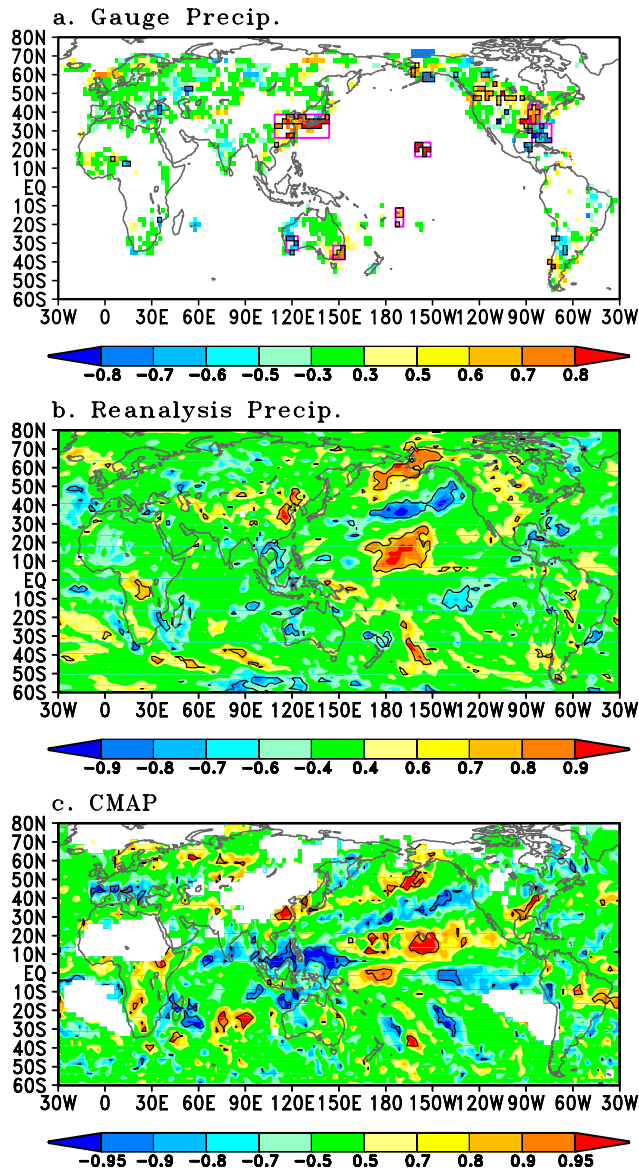


**Figure 1.**<sup>1</sup> Correlation coefficients (color) and their 95% confidence levels (black grid-box boundaries for panel *a* and contours for panels *b* and *c*) between NPI and gauge precipitations from 1930–1995 (*a*), NCEP/NCAR reanalysis precipitations from 1949–2000 (*b*), and CMAP from 1979–1999 (*c*). The 10–30-yr bandpass filter was applied to both the NPI and precipitations before calculating correlations. The color scales are chosen so that the same colors are assigned to the approximately same level of the significance, since correlations for a shorter length data generally tend to be larger than correlations for a longer length data. White color indicates the area where data are not continuously available throughout the respective periods for the correlation calculation or where data are constantly zero. The latter is the case for most of white color grids of CMAP correlations. The magenta boxes in panel *a* indicate the areas, over which area-averaged precipitation time series are calculated and their coherencies with the NPI are shown in Fig. 2.

<sup>1</sup> The larger version of Figure 1 is available from the GRL online.

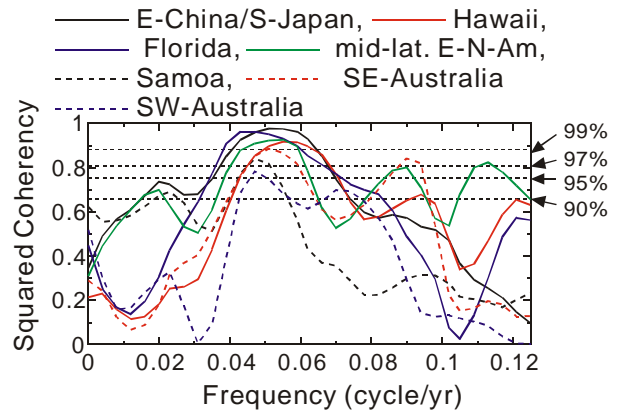


**Figure 2.** Squared coherency between the NPI and area-averaged gauge precipitation time series from 1900–1995 over eastern-China/southern-Japan (26.25°–38.75°N, 108.75°–143.75°E; solid black line), Hawaii (16.25°–23.75°N, 151.25°–161.25°W; solid red line), Florida (23.75°–33.75°N, 73.75°–86.25°W; solid blue line), and mid-latitude eastern North America (33.75°–43.75°N, 81.25°–88.75°W; solid green line), Samoa Islands (11.25°–21.25°S, 168.75°–173.75°W; dashed black line), southeastern Australia (31.25°–38.75°S, 146.25°–153.75°E; dashed red line), and southwestern Australia (26.25°–33.75°S, 116.25°–123.75°E; dashed blue line).

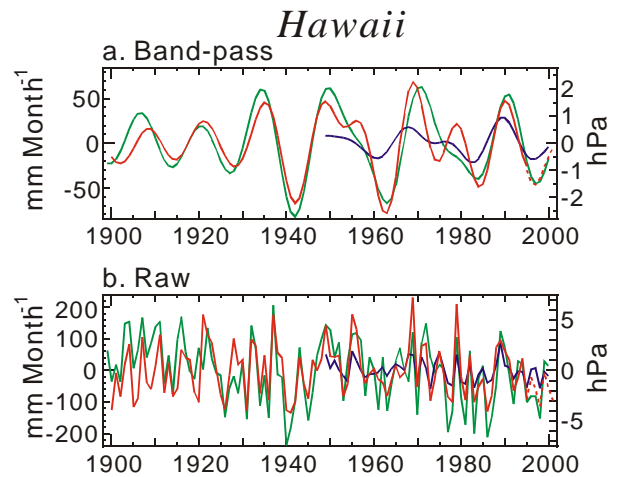


**Figure 3.** Precipitation time series of Hawaii averaged for gridded gauge data (solid red line), which is extended from 1995–2001 by the average of three gauge-measurement stations (Honolulu, Lihue and Hilo) collected in *World Monthly Surface Station Climatology* produced by the National Climate Data Center (dashed red line), and the reanalysis data (blue line), along with the NPI (green line, right-hand axis). The gauge observations and reanalysis precipitations suggest that the condition of below-normal precipitations has continued from the mid 1990s to the present in association with the BDO.

### Discussions

The bidecadal precipitation changes may have substantial socio-economic impacts, and a prime example is found for Hawaii droughts. Hawaiian Islands have been prone to droughts and water shortages, fueled by growing population. The occurrences of Hawaii droughts exhibited an interesting long-term modulation in recent decades; frequent droughts were recorded from 1975–1985 and after 1996 to the present,

but droughts were absent for the period from 1986–1995 (*personal communication, Commission of water resource managements* <http://www.state.hi.us/dlnr/cwrm/hdp/>). These periods of frequent (absent) droughts correspond to the periods of smaller (larger) precipitations in Hawaii associated with the BDO (Fig. 3), suggesting that the BDO has influenced the occurrence of Hawaiian droughts.

The fact that the most well-organized bidecadal precipitation changes occurred over the ocean suggests that the BDO in precipitations substantially influences fresh water and salinity distributions in the Pacific Ocean. Recent studies detected decadal salinity changes in the basin, such as 1980s salinity decrease in the Gulf of Alaska [Overland *et al.*, 1999], simultaneous increase in the western tropical Pacific [Suga *et al.*, 1999], and decadal salinity changes around Hawaii [Lukas, 2001]. These salinity changes may be related to the precipitation changes on decadal to interdecadal timescales. The salinity changes, in turn, might influence the relation between the temperature and density, and temperature anomalies on density surfaces can be an important factor for a mechanism of decadal variability in the atmosphere and ocean [Schneider, 2000].

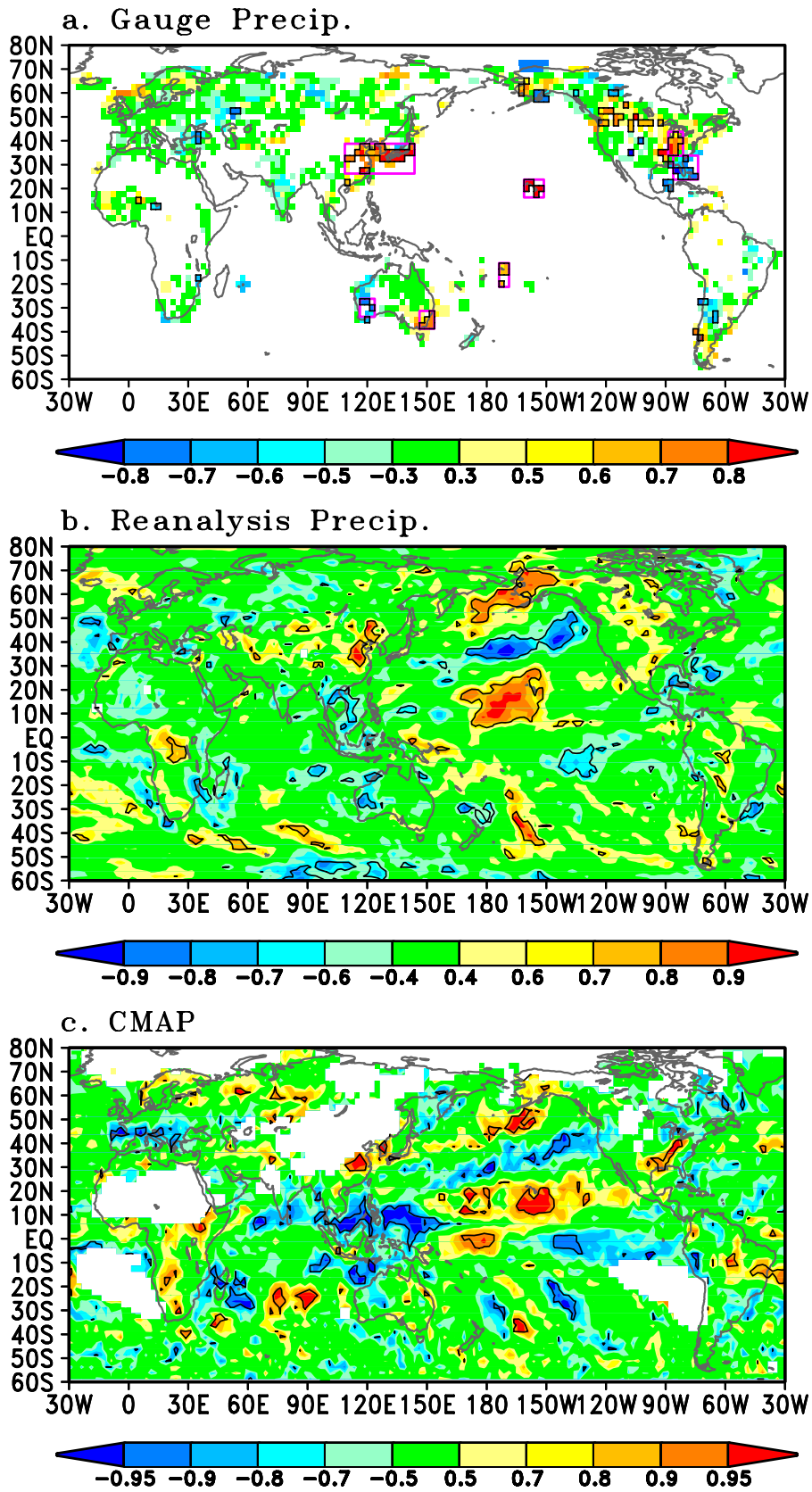
Due to the limitation of observed salinity information in the Pacific Ocean on the interdecadal timescale, one cannot fully understand the roles of the salinity changes in the ocean and further in the atmosphere based on observations. Therefore, it is important to estimate the salinity changes in numerical ocean models with careful comparisons with available salinity observations. The overall consistency of the reanalysis precipitation and gauge and CMAP data suggests that the reanalysis precipitation and evaporation can be used for a boundary condition for the ocean models.

**Acknowledgements.** We thank A. Numaguchi, M. Ikeda, S.-P. Xie, and J. M. Wallace for fruitful discussions and comments, and N. Mantua and R. Lukas for preprints. This study is supported by the grant from the Japanese Ministry of Education, Culture, Sports, Science and Technology.

## References

- Cayan, D. R., M. D. Dettinger, H. F. Diaz, and N. E. Graham, Decadal variability of precipitation over western North America, *J. Climate*, **11**, 3148–3166, 1998.
- Chu, P.-S., Hawaii rainfall anomalies and El Niño. *J. Climate*, **8**, 1697–1703, 1995.
- Cook, E. R., D. M. Meko, and C. W. Stockton, A new assessment of possible solar and lunar forcing of the bidecadal drought rhythm in the western United States. *J. Climate*, **10**, 1343–1356, 1997.
- Dai, A., I. Y. Fung, and A. D. D. Genio, Surface observed global land precipitation variations during 1900–1988. *J. Climate*, **10**, 2943–2962, 1997.
- Dettinger, M. D., and D. R. Cayan, Large-scale atmospheric forcing of recent trends toward early snowmelt runoff in California. *J. Climate*, **8**, 606–623, 1995.
- Garreaud, R. D., and D. S. Battisti, Interannual (ENSO) and interdecadal (ENSO-like) variability in the Southern Hemisphere tropospheric circulation. *J. Climate*, **12**, 2113–2123, 1999.
- Ghil, M., and R. Vautard, Interdecadal oscillations and the warming trend in global temperature time series. *Nature*, **350**, 324–327, 1991.
- Higgins, R. W., and W. Shi, Dominant factors responsible for interannual variability of the summer monsoon in the southwestern United States. *J. Climate*, **15**, 759–775, 2000.
- Horel, J. D., and J. M. Wallace, Planetary-scale atmospheric phenomena associated with the Southern Oscillation. *Mon. Wea. Rev.*, **109**, 813–829, 1981.
- Hu, Q., C. M. Woodruff, and S. E. Mudrick, Interdecadal variations of annual precipitation in the central United States. *Bull. Am. Met. Soc.*, **79**, 221–229, 1998.
- Kalnay, E., M. Kanamitsu, R. Kistler, W. Collins, D. Deaven, L. Gandin, M. Iredell, S. Saha, G. White, J. Woollen, Y. Zhu, A. Leetmaa, B. Reynolds, M. Chelliah, W. Ebisuzaki, W. Higgins, J. Janowiak, K. C. Mo, C. Ropelewski, J. Wang, R. Jenne and D. Joseph, The NCEP/NCAR 40-Year Reanalysis Project. *Bull. Amer. Meteor. Soc.*, **77**, 437–472, 1996.
- Kaplan, D., and L. Glass, Understanding nonlinear dynamics. *Springer-Verlag*, pp. 420, 1995.
- Latif, M., R. Kleeman, and C. Eckert, Greenhouse warming, decadal variability, or El Niño? An attempt to understand the anomalous 1990s. *J. Climate*, **10**, 2221–2239, 1997.
- Lukas, R., Freshening of the upper thermocline in the North Pacific subtropical gyre associated with decadal changes of rainfall. *Geophys. Res. Lett.*, **28**, 3485–3488, 2001.
- Mann, M. E., and J. Park, Joint spatio-temporal modes of surface temperature and sea level pressure variability in the Northern Hemisphere during the last century. *J. Climate*, **9**, 2137–2162, 1996.
- Mantua, N. J., S. R. Hare, Y. Zhang, J. M. Wallace, and R. C. Francis, A Pacific interdecadal climate oscillation with impacts on salmon production. *Bull. Am. Met. Soc.*, **76**, 1069–1079, 1997.
- Mantua, N. J., and S. R. Hare, Pacific Decadal Oscillation. *J. Oceanogr.*, **58**, 35–44, 2002.
- Minobe, S., A 50–70 year climatic oscillation over the North Pacific and North America. *Geophys. Res. Lett.*, **24**, 683–686, 1997.
- Minobe, S., Resonance in bidecadal and pentadecadal climate oscillations over the North Pacific: Role in climatic regime shifts. *Geophys. Res. Lett.*, **26**, 855–858, 1999.
- Minobe, S., Spatio-temporal structure of the pentadecadal variability over the North Pacific. *Progr. Oceanogr.*, **47**, 99–102, 2000.
- Minobe, S., T. Manabe, and A. Shouji, Maximal wavelet filter and its application to bidecadal oscillation over the Northern Hemisphere through the 20th century. *J. Climate*, **15**, 1064–1075, 2002.
- Overland, J. E., S. Salo, and J. M. Adams, Salinity signature of the Pacific Decadal Oscillation. *Geophys. Res. Lett.*, **26**, 1337–1340, 1999.
- Ropelowski, C. F., and M. S. Halpert, Global and regional scale precipitation patterns associated with the El Niño/Southern Oscillation. *Mon. Wea. Rev.*, **115**, 1606–1626, 1987.
- Schneider, N., A decadal spiciness mode in the tropics. *Geophys. Res. Lett.*, **27**, 257–260, 2000.
- Suga, T., A. Kato, and K. Hanawa, North Pacific Tropical Water: Its climatology and temporal changes associated with the climate regime shift in the 1970s. *Progr. Oceanogr.*, **47**, 223–256, 2000.
- Tourre, Y. M., B. Rajagopalan, Y. Kushnir, M. Barlow, and W. B. White, Patterns of coherent decadal and interdecadal climate signals in the Pacific basin during the 20th century. *Geophys. Res. Lett.*, **28**, 2069–2072, 2001.
- Trenberth, K. E., and D. A. Paolino, The Northern Hemisphere sea-level pressure data set: Trends, errors, and discontinuities. *Mon. Wea. Rev.*, **108**, 855–872, 1980.
- Trenberth, K. E., and J. W. Hurrell, Decadal atmosphere-ocean variations in the Pacific. *Clim. Dyn.*, **9**, 303–319, 1994.
- White, W. B., and D. R. Cayan, Quasi-periodicity and global symmetries in interdecadal upper ocean temperature variability. *J. Geophys. Res.*, **103** (C10), 21335–21354, 1998.
- Xie, P., and P. A. Arkin, Global precipitation: A 17-year monthly analysis based on gauge observations, satellite estimates, and numerical model outputs. *Bull. Met. Am. Soc.*, **78**, 2539–2558, 1997.
- Xie, S.-P., W. T. Liu, Q. Liu, and M. Nonaka, Far-reaching effects of the Hawaiian Islands on the Pacific ocean-atmosphere system. *Science*, **292**, 2057–2060, 2001.
- S. Minobe, Division of Earth and Planetary Sciences, Graduate School of Science, Hokkaido University, Sapporo 060-0810, Japan. (e-mail: minobe@ep.sci.hokudai.ac.jp)

(Received November, 27, 2001; revised, February, 2, 2002 ; accepted, February, 17, 2002)



LARGER-SIZE VERSION OF FIGURE 1. MINOBE AND NAKANOWATARI (FOR THE GRL ONLINE)

